JOINT EUROPEAN TORUS JET

JET–P(11)36

H.P. Summers, K. Behringer, L. Wood

Recombination of Neon-Like and Adjacent Ions in Plasmas

Recombination of Neon-Like and Adjacent Ions in Plasmas

H.P. Summers[1], K. Behringer, L. Wood[2]

JET-Joint Undertaking, Culham Science Centre, OX14 3DB, Abingdon, UK

[1]On leave of absence from Strathclyde University, Glasgow, Scotland
[2]Department of Applied Mathematics, St Andrews University, Scotland

Preprint of Paper to be submitted for publication in
Physica Scripta

1. INTRODUCTION

This paper presents preliminary results from a new comprehensive calculation of effective recombination rate coefficients for electrons and ions in finite density plasma. The principal point at issue is the dielectronic component of the effective recombination and it is this which is emphasised here.

The modern viewpoint of dielectronic recombination commences with the paper of Burgess (1964). Burgess (1965) also provided a 'General Formula' for the total dielectronic recombination coefficient, valid in the zero density limit, of great simplicity. It, and variants, have been widely used to the present time. A number of points arise. Firstly, the dielectronic coefficient is sensitive to the density of the plasma so that a density correction to the General Formula is required (Burgess & Summers, 1969). Secondly there is the question of the intrinsic accuracy of the atomic cross-section assumptions made in deriving the General Formula. It has been pointed out that the General Formula appears to overestimate when the target ion transition involved is of type $\Delta n \geq 1$ (Mertz et al, 1976). Thirdly there are omitted effects such as alternative Auger channels (Jacobs et al 1977). Finally, the role of metastable states in the recombining and recombined ion is generally ignored.

Some of these aspects have been examined selectively in other works. The present calculation takes account of all these principal phenomena in an integrated computation. It separates into four main parts:

(a) Calculation of good quality atomic excitation data for dielectronic capture to high levels,

(b) Refined calculation of direct dielectronic and radiative recombination coefficients to the lowest levels,

(c) The doubly excited population structure calculation,

(d) The singly excited population structure calculation.

Each part requires extensive numerical calculation, executed on IBM and CRAY computers. They will be summarised in Section 2.

The application in this paper is to the neon-like and adjacent stages of transition metals, Cr, Fe and Ni. These elements are important impurities in the JET tokamak (Cr, Ni) or important in other or future tokamaks. Also we shall show some results for dielectronic recombination to form neon-like selenium (Se^{+24}) of interest for X-ray laser studies. The results and discussion are in Section 3.

2. THE CALCULATION

2.1 Outline and nomenclature

Recombination commences with a z-times ionised ion A^{+z}. The states of A^{+z} may be denoted by $A^{+z}(p)$ which we call the parent ion states. In a plasma, to high probability, initially A^{+z} is in its ground state or a metastable state denoted by p_0 (Greek suffices). Direct radiative recombination forms a state $A^{+z-1}(p_0,n\ell)$ based on the initial parent. States based on ground or metastable parents are called singly excited.

True excited states of A^{+z} are denoted by p_i (Roman suffices). Direct dielectronic recombination forms initially, by resonant capture, a state based on an excited parent $A^{+z-1}(p_i,n\ell)$ which can autoionise. These are called doubly excited states and can stabilise radiatively to singly excited states. Doubly excited state populations in a plasma are affected by collisions with plasma electrons and ions. The main result is to cause ℓ redistribution which alters the Auger/radiative stabilisation branching. The solution of the redistribution and the deduction of the resultant direct

dielectronic recombination to singly excited states is called the doubly excited population structure calculation.

Singly excited states with outer electron in high excited orbitals are vulnerable to collisional ionisation and redistribution. Thus all direct captures do not lead to population of the ground or metastable states of A^{+z-1}. The calculation of the singly excited state populations in a plasma and the consequential effective recombination coefficients (the 'collisional-dielectronic recombination coefficients') is called the singly excited population structure calculation.

Direct recombination into n=3 levels for the ions considered in this paper requires special study. Refined calculation is required in this case both for dielectronic and radiative recombination due to the large quantum defects and the interference between captured and parent electrons. This is called the low level problem. Direct recombination into n>3 levels is called the high level problem. There are infinitely many such levels and up to n~500 may need to be considered at low density to obtain converged final results. Such levels are close to their parent continua and thus other techniques may be used for calculation of direct capture involving them.

The typical energy level pattern is shown in figure 1 for $Fe^{+17} + e \rightarrow Fe^{+16}$ recombination. The initial parent state is the fluorine-like ground state $2s^2 2p^5\ ^2P$. The low doubly excited states are shown enclosed in a dashed line. Each block shows the span in energy of terms belonging to the indicated configurations. There are many such terms.

Populations are treated at various degrees of angular resolution, such as p,nℓS with total spin specified or p,n, that is summed over total spin and ℓ. The behaviour of the population densities in the plasma is most usefully described by the Saha-Boltzman deviation factors $b(p_\sigma;\ p_\rho, n\ell S)$. Direct dielectronic recombination is denoted

by, eg, $\alpha_d(p_0; p_\rho, n\ell S)$. These notations indicate the initial capturing parent, p_0, and the final singly excited state at a particular resolution, $p_\rho, n\ell S$.

2.2 Low level dielectronic and radiative recombination

Auger and spontaneous rates are calculated in a multiconfiguration, multielectron perturbative approximation. This is based on distorted wave orbitals in a scaled Thomas-Fermi-Dirac potential (Badnell, 1985; Eissner et al, 1973). Combination of rates to form n=3 doubly excited populations and resultant direct dielectronic recombination coefficients is performed automatically.

The total direct dielectronic recombination via low doubly excited states for $Se^{+25} + e \rightarrow Se^{+24}$ is shown in figure 2. The total is separated into proportions occurring through the possibly doubly excited configurations. These configurations are the same as shown for $Fe^{+17} + e$ in figure 1. LS coupling without relativistic interactions was adopted in the results shown. The component direct dielectronic recombination coefficients to the bound excited LS terms of Se^{+24} are shown in figure 3. The results for the 3d terms are not shown.

Radiative recombination to low levels is calculated using the techniques described in detail by Summers (1986)

2.3 High level dielectronic recombination and doubly excited population structure

Auger rates are deduced from analytic continuation of distorted wave partial collision strengths to below threshold. Accurate partial waves are central to the derivation of reliable Auger rates. For $\Delta n=1$ parent transitions, direct dielectronic recombination to low ℓ states is sensitive to the associated Auger rates and low ℓ capture constitutes the major portion of the total dielectronic capture. It is approximations for Auger rates in these cases which are responsible for inaccuracy in the

General Formula. We calculate all required partial wave collision strengths for each parent transition explicitly. Automatic comparison with Bethe approximation partial collision strengths is performed for dipole transitions. These comparisons are relevant to revision of the General Formula and will be given elsewhere. Non-dipole parent transitions are also calculated. Data for all alternative Auger pathways are evaluated. Thresholds for opening of autoionising levels are obtained with some precision using quantum defect expansion and static dipole polarisabilities. All dipole ℓ changing (n fixed) collisional transitions by electrons and positive ions are included in the doubly excited population structure determination. The plasma ions are treated as a single species of effective charge Zp. It is these positive ions which are primarily responsible for the redistribution. Resolution into spin systems is relevant for doubly excited populations of neon-like and magnesium-like ions.

2.4 Collisional-dielectronic coefficients and singly excited population structure

The techniques of section 2.2 and 2.3 provide refined direct dielectronic and radiative recombination coefficients onto singly excited states. All radiative transitions and collisionally induced transitions by impact of plasma electrons and positive ions are included in the subsequent singly excited population structure calculation. These procedures have been described by Burgess and Summers (1976), Summers (1977) and Spence and Summers (1986). Arbitrary angular resolution of populations is possible and both 'collisional-dielectronic' and 'generalised collisional-dielectronic' coefficients can be produced. These procedures include metastable states consistently. However for the recombining ions considered in this paper metastable states are not important. Ground state parents of singly excited states only therefore need to be treated. Also since it is the effective recombination coefficients which are principally sought, full angular resolution of singly excited

populations is not required. Complete ℓ redistribution occurs at principal quantum levels n lower than those subject to collisional ionisation. For recombined neon-like and magnesium-like ions, the recombination into the separate spin systems is potentially of interest. Evidently recombination on the triplet side accumulates on the triplet metastable stage, whereas recombination on the singlet side accumulates on the ground state. Spin system mixing occurs, however it will be shown from the doubly excited population solution that the ratio of effective recombination coefficients into singlet and triplet metastables are simple. For these reasons, the most general operation of the population codes is not warranted by the present ion selection. Results in the general case will be given elsewhere.

3. RESULTS AND DISCUSSION

Figure 4 shows the high level doubly excited populations based on the $2s^22p^6$ 3p parent in dielectronic capture by Cr^{+13} (sodium-like). The $2s^22p^6$ 3s, $2s^22p^6$ 3p and $2s^22p^6$ 3d parent terms are included in the calculation. The curves for n=6, 7 and 8 are notable. Resonant capture through the parent transition $2s^22p^6$ 3s - $2s^22p^6$ 3p opens only for $n \geq 9$. The population of n=6, 7, 8 is due to the non-dipole parent excitation $2s^22p^6$ 3s - $2s^22p^6$ 3d followed by parent core radiative transition. The underpopulation of n=8 is due to the opening of the $2s^22p^6$ 3d nℓ → $2s^22p^6$ 3p kℓ'Auger channel. For $n \geq 9$, the usual strong dipole parent excitation channel opens and the b-factors are very close to unity to quite large ℓ. The effect of plasma density is also shown, which is redistribution to higher ℓ. Figure 5 shows the consequential effect on the direct dielectronic recombination to singly excited levels. The density dependent increase is quite significant at Tokamak densities. Excited states n<6 are not accessible via this group of parent transitions.

Figure 6 shows direct dielectronic and radiative recombination coefficients to n shells in capture by N_i^{+18}

(neon-like). The parent configurations have been treated in three groups for the three principal $\Delta n=1$ transitions active, namely, 1) $2s^22p^6$, $2s^22p^5$ 3s (3 terms), 2) $2s^22p^6$, $2s^22p^5$ 3d, $2s^22p^5$ 3p (13 terms), 3) $2s^22p^6$, $2s^22p^6$ 3p, $2s^22p^5$ 3p, $2s^22p^6$ 3s (11 terms). Low n=3 levels are open for dielectronic capture. The n=3 values for direct radiative and dielectronic recombination are calculated in the refined low level treatment. All initial parent transitions are of $\Delta n=1$ type, so that the direct dielectronic recombination coefficients fall quite rapidly with increasing n. Doubly excited state redistribution has only a small effect at typical tokamak plasma densities.

Figure 7 shows the direct dielectronic and radiative coefficients to nS shells in capture by N_i^{+17} (sodium-like). Both $\Delta n=0$ and $\Delta n=1$ initial parent transitions are present and are of markedly different behaviour. The parent groupings are 1) $2s^22p^6$ 3s, $2s^22p^6$ 3p, $2s^22p^6$ 3d (3 terms), 2) $2s^22p^6$ 3s, $2s^22p^5$ $3s^2$ (2 terms), 3) $2s^22p^6$ 3s, $2s^22p^5$ 3s3d, $2s^22p^6$ 3d, $2s^22p^5$ 3s3p (20 terms), 4) $2s^22p^6$ 3s, $2s2p^6$ 3s3p, $2s^22p^5$ 3s3p, $2s2p^6$ $3s^2$ (14 terms). Type 1) singlet and triplet contributions are exactly in 1:3 ratio. The difference observed in the low level n=3 direct dielectronic recombination between singlet and triplets might have been expected on exclusion principle grounds. The effect of alternate Auger pathways in type 4) is marked but as a whole this parent group is not a major contributor to the net capture.

Figure 8 shows the singly excited population structure of N_i^{+17} and figure 9 that of N_i^{+16}. Figure 8 emphasises temperature behaviour and figure 9 density behaviour. The collisional-dielectronic recombination coefficient, α_{cd}, is also given. The effect of increasing temperature is a broad rise of all b-factors, whereas the effect of increasing density is a progressive erosion of the high n b-factors. The effect of plasma density is marked only in $N_i^{+17} + e \rightarrow N_i^{+16}$ recombination where highly excited n shells are

populated by dielectronic recombination via $\Delta n=0$ parent transitions. For $\Delta n=1$ parent transitions for the present ions, the density effect is much smaller at tokamak densities. At the electron temperatures given in figure 8, the effective recombination coefficients are in the vicinity of the peak due to dielectronic recombination. The breadth of the peak from the present results is greater than would be obtained from the General Formula with a single effective parent transition. This is due to the importance of $n=3$ capture and the precise resonant energies used here.

4. CONCLUSIONS

A new detailed calculation of effective electron-ion recombination in plasmas has been presented which takes account of all major effects. The role of metastables is incorporated fully in the model but is not required for the present selection of ions.

The results given here are preliminary and selective. They indicate the trend of effects but should not be used for overall scaling of simpler general treatments. Detailed comparisons will be published elsewhere.

Doubly excited state redistribution is significant at tokamak densities for the present ions when $\Delta n=0$ parent transitions are possible in the dielectronic process.

Density dependent reduction of the effective recombination coefficient is substantial at tokamak densities (~ factor 2) when $\Delta n=0$ parent transitions are present.

The ratios of distorted wave to Bethe partial collision strengths obtained in the course of this work indicate that the mean universal ratios implicitly used in the General Formula are somewhat too large for $\Delta n=1$ parent transitions for the present ions. The broad consequence is a reduction

in dielectronic coefficients for $\Delta n=1$ parent transitions at zero density over those given by the General Formula. Note however that use here of precise resonant energies especially for low doubly excited states means that a single temperature independent scaling is not a proper 'correction' to the General Formula.

Non-dipole parent transitions are significant in some cases. Alternative Auger pathways occur but are not of great significant for the ions examined here.

5. CONSEQUENCES FOR TOKAMAK DIAGNOSTICS

The radial distribution of the number density of neon-like and sodium-like nickel and chromium and the radial distribution of radiation of the sodium-like ions are of considerable interest in the JET plasma (Behringer et al, 1986). Theoretical calculations of these profiles requires not only reliable effective recombination coefficients as investigated here, but also ionisation and transport coefficients. The prescription for ionisation followed by us is that of Burgess & Chidichimo (1983). For ionisation of sodium-like chromium and nickel, a portion of the ionisation occurs through inner shell (2s and 2p) excitation to autoionising levels which in the prescription are assumed to autoionise with unit probability. Our calculations here indicate that the branching ratio for autoionisation (against radiative stabilisation) is of order ½. Figure 10 shows the trend of these effects on the theoretical radial shell structure of nickel ions for a particular JET pulse. The initial rate coefficient data set for neon-like - sodium-like nickel, with results given by solid lines, have been uniformly scaled to match the new data at 300 eV (100 cm). It is evident that transport is a major factor, along with ionisation and recombination. The new results show an increase in peak N_i^{+17} fractional abundance (total nickel =

1.2 in the units of figure 10) while the shell width is little altered. This implies revision of nickel abundance determination from integrated N_i^{+17} line emission.

ACKNOWLEDGEMENTS

We are greatly indebted to Dr N Badnell for allowing use of his AUTOSTRUCTURE code, and to Dr H E Mason for assistance in implementing the University College, London SUPERSTRUCTURE and distorted wave codes on our computer systems.

REFERENCES

Badnell N R (1985) Cambridge University, Applied Mathematics Department Report, DAMPT/AA/-1001-NRB

Behringer K H, Carolan P G, Denne B, Decker G, Engelhardt W, Forrest M J, Gill R, Gottardi N, Hawkes N C, Kallne E, Krause H, Magyar G, Mansfield M, Mast F, Morgan P, Peacock N J, Stamp M F, Summers H P (1986) Nuclear Fusion 25, 751

Burgess A (1964) Astrophys. J. 139, 776

Burgess A (1965) Astrophys. J. 141, 1598

Burgess A & Chidichimo M (1983) Mon. Not. R. Astr. Soc. 203, 1269

Burgess A & Summers H P (1969) Astrophys. J. 157, 1007

Burgess A & Summers H P (1976) Mon. Not. R. Astr. Soc. 174, 345

Eissner W, Jones M & Nussbaumer H (1974) Computer Phys. Commun. 8, 270

Jacobs V L, Davis J, Kepple P C and Blaha M (1977) Astrophys. J. 211, 605

Mertz A L, Cowan R D and Magee N H (1976) Los Alamos Laboratory report, LA-6220-MS

Post D E, Jensen R V, Tarter C B, Grasberger W H and Lokke W A (1977) At. Data Nucl. Data Tables 20, 397

Spence J & Summers H P (1986) JET Joint Undertaking report JET-P(86)Ø1
(J. Phys. B. - in press)

Summers H P (1977) Mon. Not. R. Astr. Soc. 178, 101

Summers H P (1986) JET Joint Undertaking report, JET-P(86)Ø7
(Mon. Not. R. Astro. Soc. - in press)

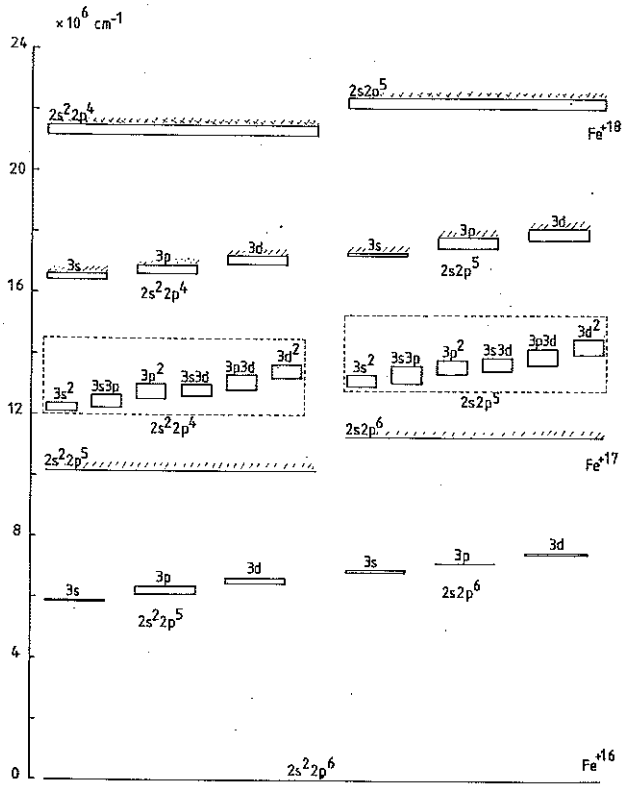

Fig. 1 Energy diagram of configurations involved in the dielectronic recombination $Fe^{+17} + e \rightarrow Fe^{+16}$. Hatching indicates the parent states. The low (n=3) doubly excited states of Fe^{+16} are enclosed by a dashed line.

P(86)36

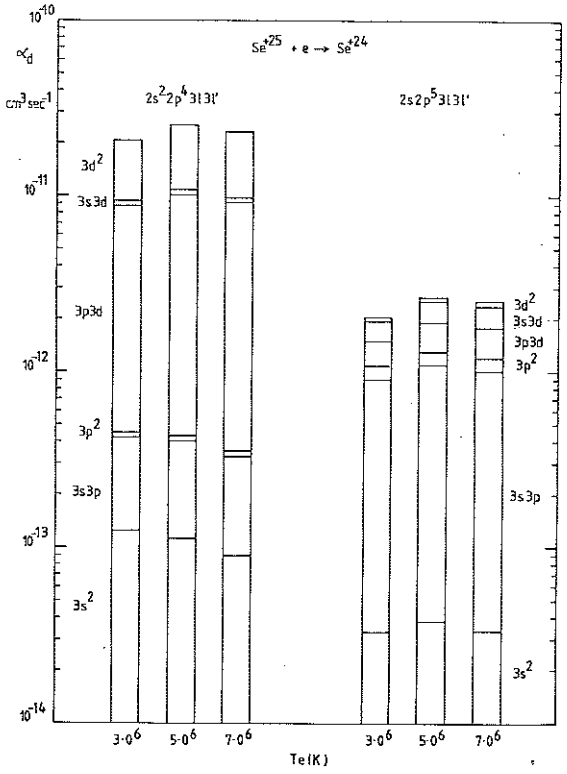

Fig. 2 Proportions of the total dielectronic recombination $Se^{+25} + e \rightarrow Se^{+24}$ through low (n=3) doubly excited states from the separate doubly excited states.

P(86)36

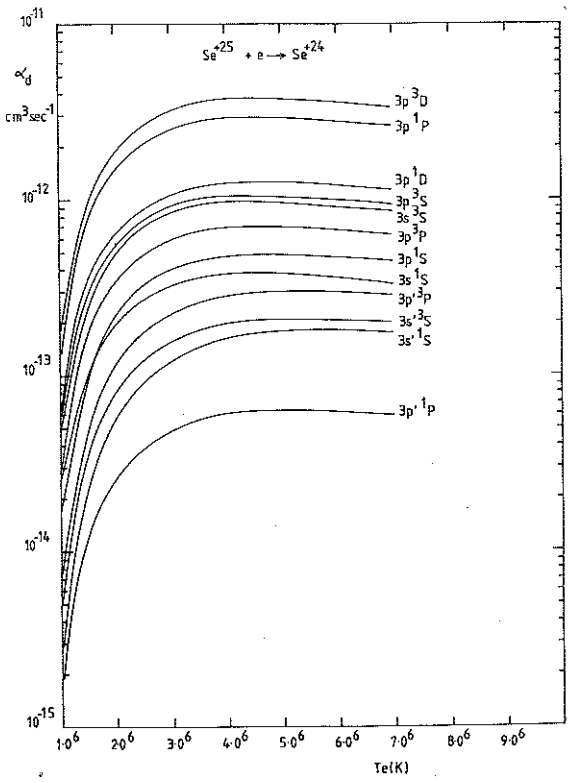

Fig. 3 Proportions of the total dielectronic recombination $Se^{+25} + e \rightarrow Se^{+24}$ through low (n=3) doubly excited states into n=3 bound terms.

P(86)36

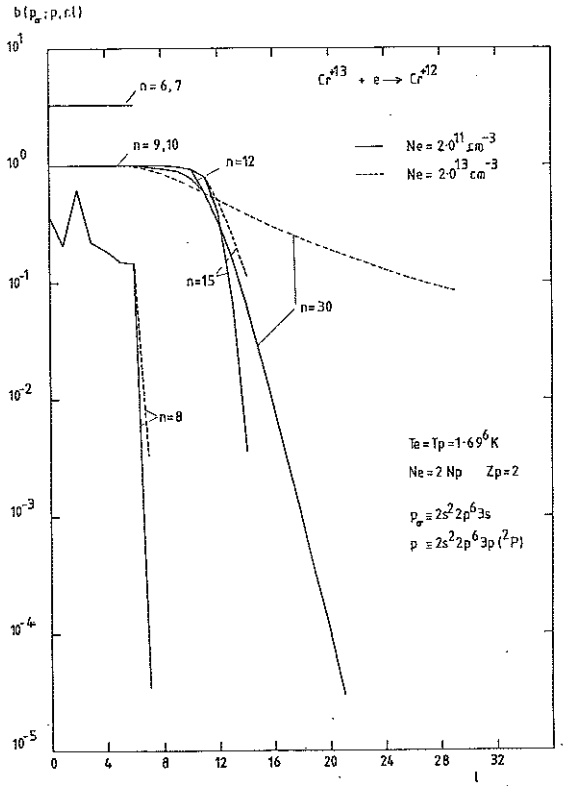

Fig. 4 Doubly excited population structure in the dielectronic recombination $Cr^{+13} + e \rightarrow Cr^{+12}$. Parent configurations included are $2s^2 2p^6$ 3s, $2s^2 2p^6$ 3p and $2s^2 2p^6$ 3d. Ne is the electron density, Te the electron temperature, Np the mean ion density, Tp the mean ion temperature, Zp the mean ion charge.

P(86)36

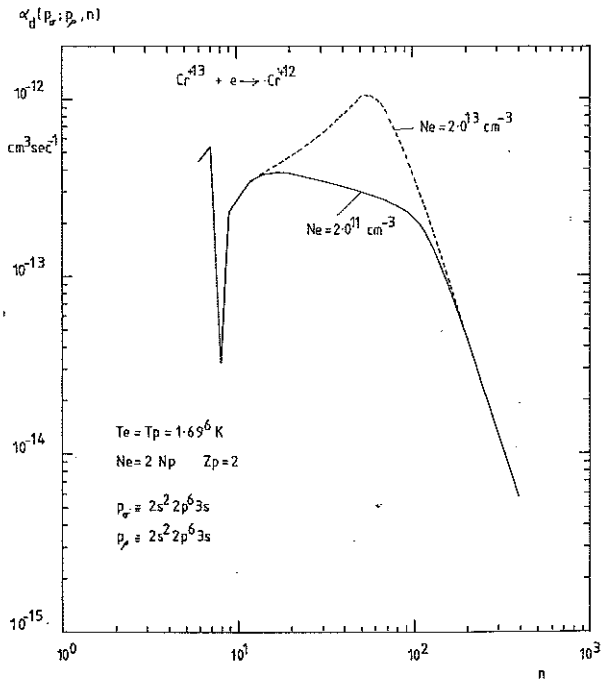

Fig. 5 Direct dielectronic recombination to n shells for $Cr^{+13} + e \rightarrow Cr^{+12}$. Parent configurations included are $2s^2 2p^6$ 3s, $2s^2 2p^6$ 3p and $2s^2 2p^6$ 3d.

P(86)36

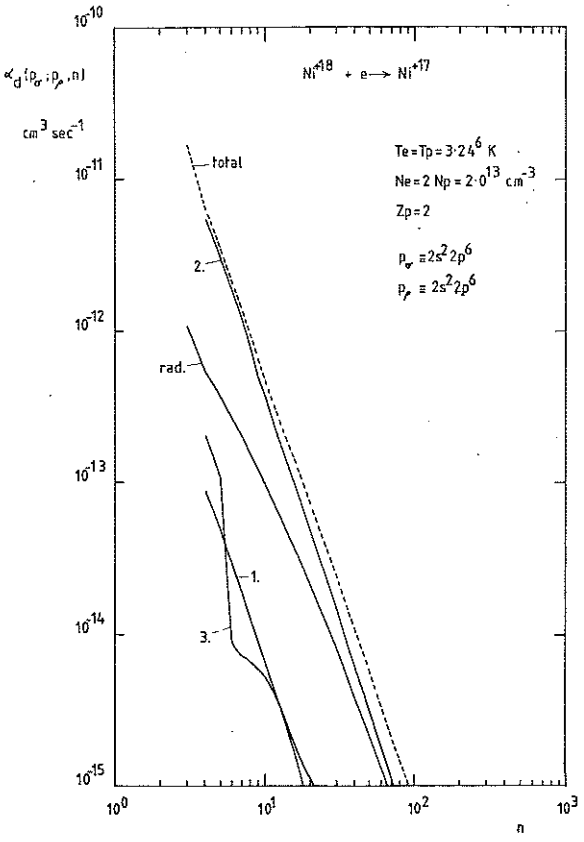

Fig. 6 Direct dielectronic recombination to n shells for $N_i{}^{+18} + e \rightarrow N_i{}^{+17}$. Contributions to the total arise from parent configurations:

1) $2s^2 2p^6$, $2s^2 2p^5$ 3s,

2) $2s^2 2p^6$, $2s^2 2p^5$ 3d, $2s^2 2p^5$ 3p

3) $2s^2 2p^6$, $2s2p^6$ 3p, $2s2p^6$ 3s, $2s^2 2p^5$ 3p.

The low level treatment is used for n = 3.

P(86)36

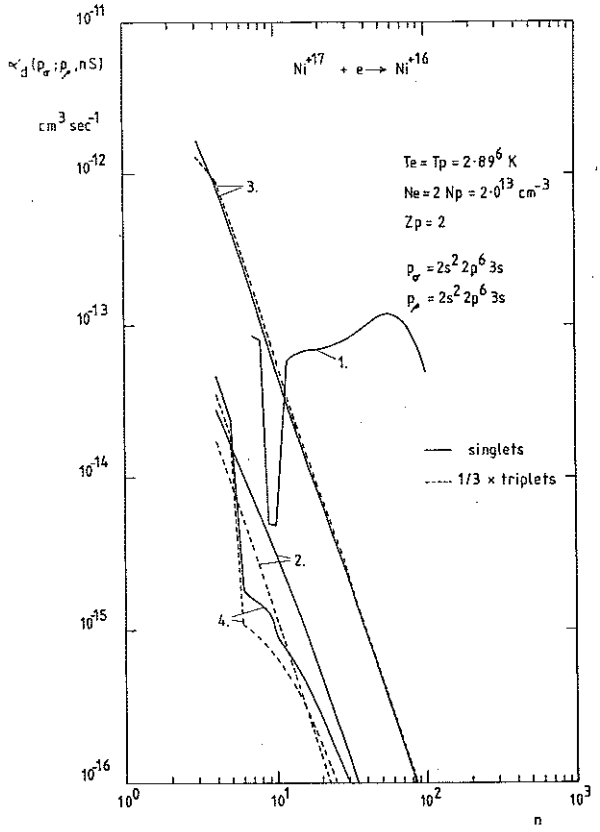

Fig. 7 Direct dielectronic recombination to nS shells for $N_i^{+17} + e \rightarrow N_i^{+16}$. Contributions to the total arise from parent configurations:

1) $2s^2 2p^6$ 3s, $2s^2 2p^6$ 3p, $2s^2 2p^6$ 3d
2) $2s^2 2p^6$ 3s, $2s^2 2p^5$ $3s^2$
3) $2s^2 2p^6$ 3s, $2s^2 2p^5$ 3s3d, $2s^2 2p^6$ 3d, $2s^2 2p^5$ 3s3p
4) $2s^2 2p^6$ 3s, $2s2p^6$ 3s3p, $2s^2 2p^5$ 3p, $2s2p^6$ $3s^2$

Singlets and triplets are not distinguishable for case 1).

P(86)36

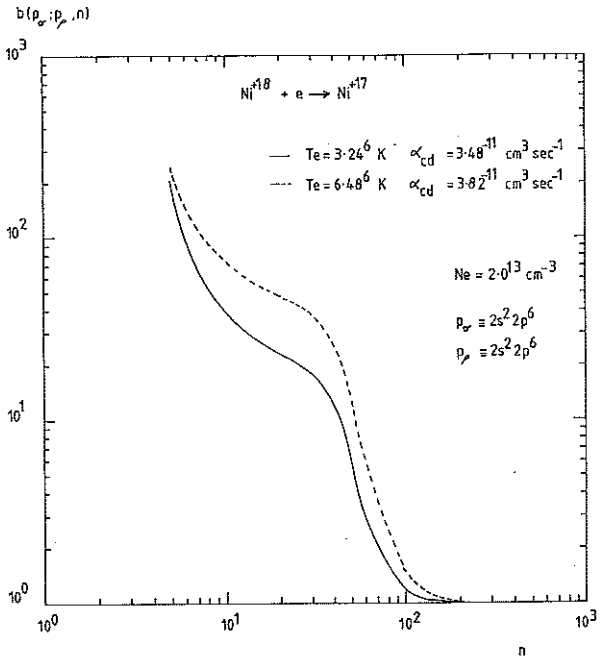

Fig. 8 Singlet excited population structure of n shells in the recombination $N_i^{+18} + e \rightarrow N_i^{+17}$. α_{cd} is the collisional-dielectronic recombination coefficient.

P(86)38

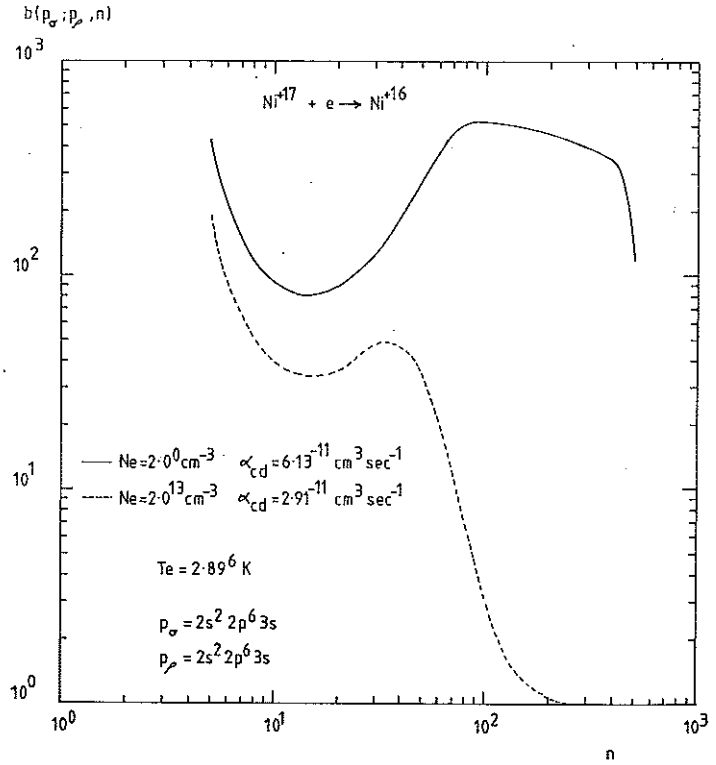

Fig. 9 Singly excited population structure of n shells in the recombination $N_i^{+17} + e \rightarrow N_i^{+16}$.

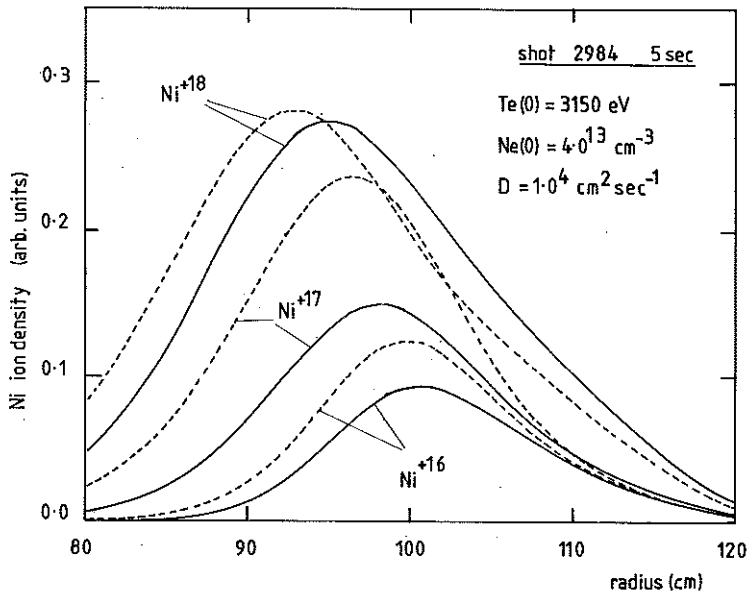

Fig. 10 Theoretical radial distribution of nickel ion abundances across the JET torus from the recombination and diffusive transport model.

——— S calculated according to Burgess-Chidichimo, α calculated according to General Formula with Mertz (1976) and density (Post et al. 1977) corrections.

— — — — adjusted neon-like - sodium-like α and S.